6th IEEE RAS/EMBS International Conference on
Biomedical Robotics and Biomechatronics (BioRob)
June 26-29, 2016. UTown, Singapore

Effect of anodal tDCS on human prefrontal cortex observed by fNIRS*

M. Raheel Bhutta, Seong-Woo Woo, M. Jawad Khan, Keum-Shik Hong, *Senior Member, IEEE*

Abstract— **Transcranial direct current stimulation (tDCS) is one of the noninvasive brain stimulation methods that have been used to study many neuropsychiatric and neurological disorders in humans. tDCS can excite or inhibit the neurons depending upon its polarity. In this study, we have investigated the effect of anodal tDCS on human prefrontal cortex using functional near-infrared spectroscopy (fNIRS), which is a noninvasive neuroimaging technique. We have developed a new wireless fNIRS system compatible with EEG, and also developed a pad-type tDCS with variable current limits. Our wireless fNIRS system is composed of a microcontroller, an optical probe, tri-wavelength light emitting diodes (LEDs), photodiodes, WiFi communication module and battery. The developed tDCS system can generate the current in the range of 0.8 ~ 2.2 mA. To test the functionality of the systems, fNIRS data was recorded before and after the tDCS stimulation. The results of this study show that the anodal tDCS excites the neurons in the region of interest and this excitability is monitored using the fNIRS system.**

I. Introduction

In the recent past, extensive research has been done to study the brain behavior and to treat a number of neuropsychiatric and neurological disorders by applying the noninvasive neurostimulation methods. The two most common techniques used for noninvasive neurostimulation are: transcranial magnetic stimulation (TMS) and transcranial direct current stimulation (tDCS). In TMS a strong brief electrical current is passed through an insulated wire coil placed on the skull. This current flow generates a transient magnetic field which induces a secondary current in the brain. This induced current depolarizes the neurons, and more neurons are made to fire [1]. Whereas in tDCS a low-intensity constant direct current (0.5 ~2 mA) is applied to the scalp of the target region using the electrodes (surface area of 20 ~ 35 cm2). By applying the tDCS neurons can be de- or hyper-polarized depending upon the polarity of tDCS. Anodal tDCS excites the working of neurons whereas the cathodal tDCS inhibits the working of the targeted neurons. TMS has better temporal and spatial resolution but TMS systems are very expensive and difficult to operate whereas tDCS has the advantage of easier to use, and easier to apply concurrently with behavioral tasks [2-3].

fNIRS is a noninvasive, brain imaging technique that is recently been used a lot for regional measurement of the oxygenation of hemoglobin in body's tissue [4-8]. fNIRS can measure the concentrations of oxy-hemoglobin (HbO) and deoxy-hemoglobin (HbR) by observing the absorption of the near-infrared light at particular wavelengths. Both HbO and HbR have different absorption of the right, spectroscopy techniques can be used to provide an index of blood oxygenation and hence oxygen delivery. So fNIRS give us proportionally exact concentration data of oxygenated hemoglobin. fNIRS is able to detect even small changes in the cerebral hemodynamic response to functional stimulation with noninvasive way [9-11]. The capability of fNIRS to measure the hemodynamic change related to the human brain activities, such as motor, visual, auditory, language, other cognitive functions was described in several reports [12-16]. Different methods of fNIRS are utilized in several areas such as neuroscience [17-19], sports medicines [20], clinical [21], neuropsychology [22-24] and brain-computer-interface (BCI) [25-28], applications.

In this study, we have investigated the effect of anodal tDCS on human prefrontal cortex using fNIRS. To complete our objective we have developed a small portable fNIRS system with a pad-type tDCS with variable current limits. The developed fNIRS system has flexible probe which can accommodate the sensors from EEG system as well in future. The system functionality was tested using three male subjects and fNIRS recording before and after the current stimulation. The results show that the anodal tDCS excites the neurons under the stimulation region.

II. Instrumentation

A. fNIRS Development

The hardware of the fNIRS system consists of two major parts: (i) data acquisition module (ii) data processing module.

The major responsibilities of the data acquisition module are to control the sequence of light emission to the subject body and then enabling of respecting photodiode to detect the scattered light. This module is also responsible for transmitting the collected data to the data processing module. Data acquisition module consists of two main parts: (a) flexible optical probe, which has the holes in which light sources and detectors can be strategically arranged as per the requirement of the experiment; and (b) a control and operation electronics, which consists of a microcontroller, drive circuitry, WiFi module, and power supply.

*Research supported by National Research Foundation of Korea under the Ministry of Science, ICT and Future Planning, Korea (grant no. NRF-2014-R1A2A1A10049727).

M. Raheel Bhutta is with the Department of Cogno-Mechatronics, Pusan National University, Busan 46241, South Korea (e-mail: cogno@pusan.ac.kr).

Seong-Woo Woo is with the School of Mechanical Engineering, Pusan National University, Busan 46241, South Korea (e-mail: swwoo@pusan.ac.kr).

M. Jawad Khan is with the School of Mechanical Engineering, Pusan National University, Busan 46241, South Korea (e-mail: jawad@pusan.ac.kr).

Keum-Shik Hong is with the School of Mechanical Engineering and Department of Cogno-Mechatronics Engineering, Pusan National University, Busan 46241, South Korea, (corresponding author, phone: +82-51-510-2454; fax: +82-51-514-0685; e-mail: kshong@pusan.ac.kr).

The flexible optical probe is made by combining the Sylgard® 184 silicone elastomer base solution with the silicon elastomer curing solution in the ratio of 10:1. The ratio between the base solution and curing solution is very important for the flexibility of the probe. By increasing the ratio of curing solution the probe can be more rigid. Some drops of black ink were included in the mixture so that the probe is made in black color to avoid the interference from the outside light on photodiodes. The holes are made in the probe according to the size of light emitting diodes (LEDs) and photodiodes. Holes are made at a distance of 2cm from each other. The total size of the probe is 20cm×5cm. There are four tri-wavelength LEDs (L735/805/850-40B32, Epitex Inc., Japan) and ten photodiodes (S1223-01, Si Photodiode, Hamamatsu Photonics, Japan) in our system. Each LED can emit light at three wavelengths 735nm, 805nm, and 850 nm. The LED has a total radiant power of 9mW at each wavelength. In our design we are using only two wavelengths (735nm and 850nm) from each LED. We have used LEDs rather than laser as light sources because, LEDs are inexpensive, easy to use and there is no need of fiber cables because LEDs can be directly attached to the human body. Each photodiode, used in our system, can detect the light of wavelength from 320 nm - 1100 nm, with an active area of 3.6 mm x 3.6 mm. The LEDs are time multiplexed and the emitted light of one wavelength from LED can be detected by all ten photodiodes so we can make a maximum of forty channels using all four sources and ten photodiodes. Uniform intensity of LEDs is controlled by the drive circuitry. The flexible probe is designed in such a way that in future it can accommodate the sensors from EEG system as well.

Control and operation electronics consists of three major parts: a microcontroller which controls all the switching of light sources and detectors, a drive circuitry which is used to power the LEDs with uniform intensity and to amplify the small signal received from the detectors, WiFi module to transmit data wirelessly, and power supply to operate all the circuits. Transimpedance circuit converts the light intensity signal detected by a photodiode into voltage. This converted signal is amplified with a flexible gain using the OP-AMP (LM324) in a non-inverting amplifier scheme. An analog to digital converter (ADC) module available in microcontroller (dsPIC33FJ256MC710A, Microchip technologies, U.S.A.) is used to digitize these amplified analog voltage values. Microcontroller is also responsible for the control of switching between the different wavelengths of LED sources and activation of photodiodes to detect the light signal. The switching mechanism is shown in Figure 1. A total of 80 data values can be collected in one sample (4 sources x 2 wavelengths x 10 detectors). The sampling rate of the system is upto 50 Hz which is enough to measure the slow hemodynamics response [29-34] and also can measure the fast neuronal response [35-36].

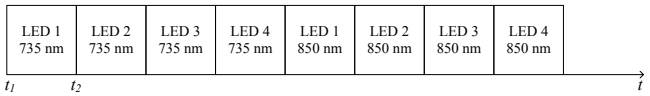

Figure 1. Time multiplexed switching sequence of LEDs

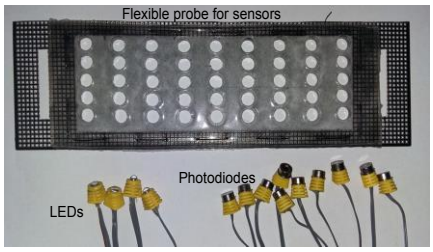

Figure 2. Flexible probe with LEDs and Photodiodes

The digitized light intensity values are then transmitted serially to an 802.11 b/g WiFi module (RN131 EK, Roving Network, U.S.A.), which transmits the data wirelessly to the data processing module. In our system we have used WiFi medium rather than any other medium like Bluetooth because it has many advantages over other mediums like: it can transmit data at a much faster speed (up to 11mbps), using WiFi we can connect multiple devices with the module at one time. Furthermore WiFi module has more coverage area than Bluetooth, also there is no need of line of sight for the WiFi devices to connect with a module so the devices at far area or even in other room can connect with a module. This advantage of WiFi is very helpful in our fNIRS system to be used in clinical environment.

The power supply circuitry was designed with special care because we need different voltages to run different circuits available in our design. In our design photodiodes and LEDs are operating at 5v whereas microcontroller board is working at 3.3v. We used a lithium-polymer battery (LiPo 12000XL 2-cell 7.4v, Maxamps, U.S.A.). To fulfill the requirements of our system (3.3v and 5v) the voltage was down regulated.

The digitized light intensity values from the data acquisition module were transmitted to the data processing module over the WiFi medium. Now-a-days all laptops and personal digital assistants (PDAs) have built in WiFI module so in our system any device can connect to our data acquisition module. We have developed a MATLAB based GUI to display the raw intensity values or raw oxy-hemoglobin values in real time. Using our GUI we can record the intensity values into a text file for future offline processing. We have also developed a separate software based on MATLAB for offline processing of data.

From the raw intensity values, the changes in optical density ΔA, can be calculated at each discrete time k,

$$\Delta A(k;\lambda) = -\ln \frac{I_{out}(\lambda)}{I_{in}(k;\lambda)} = l.D(\lambda).\Delta\mu_a(k;\lambda), \qquad (1)$$

where I_{in} is the intensity of incident light, I_{out} is the intensity of detected light, D is the differential pathlength factor (DPF), l is the distance between the emitter and the detector, and $\Delta\mu_{\text{a}}$ is the absorption change of the tissue. The changes of oxy-hemoglobin (Δc_{HbO}) and deoxy-hemoglobin (Δc_{HbR}) were measured using the modified Beer-Lambert Law [37] as:

$$\begin{bmatrix} \Delta c_{\text{HbO}}(k) \\ \Delta c_{\text{HbR}}(k) \end{bmatrix} = \begin{bmatrix} lD^{\lambda_1}\alpha_{\text{HbO}}^{\lambda_1} & lD^{\lambda_1}\alpha_{\text{HbR}}^{\lambda_1} \\ lD^{\lambda_2}\alpha_{\text{HbO}}^{\lambda_2} & lD^{\lambda_2}\alpha_{\text{HbR}}^{\lambda_2} \end{bmatrix}^{-1} \times \begin{bmatrix} \Delta A_1(k,\lambda_1) \\ \Delta A_2(k,\lambda_2) \end{bmatrix}, \qquad (2)$$

with λ_1 = 735 nm, λ_2 = 850 nm, $D^{\lambda 1}$ = 6.3125, and $D^{\lambda 2}$ = 5.235 [38], according to the values for the wavelength-dependent absorption coefficients α_{HbO}, α_{HbR} taken from UCL, Department of Medical Physics and Bioengineering website [39]. While detecting the hemodynamic response, fNIRS can also get the physiological noises like heart pulse, respiration, and low-frequency Mayer waves. We use a second-order low-pass filter with a cutoff frequency of 0.15Hz to remove these noises.

B. *tDCS Development*

We have developed a tDCS system with variable current limits. The developed tDCS can generate a constant current from 0.8 ~ 2.2 mA. To meet the requirements of our system we have used 2.2kΩ resistor (2EA), 9V power battery, 5kΩ potentiometer, and a current regulator (LM334Z). Potentiometer is a variable resistor which can control the value of incoming current. Depending upon the value of resistor the output current value also changes. The current is divided by 2 lines. One line has resistor and potentiometer, the other has only resistor. If we change the resistance of potentiometer, total resistance of the first line is changed and then current of the line is changed, too. In this sequence, range of total resistance is 2.2~7.2 kΩ. Like this reason, we can modulate the current more accurately. The functionality of current regulator is to stabilize the current. If output current has irregular fluctuations, current regulator tries to filter those fluctuations so that we can get smooth current at the output.

III. EXPERIMENTAL SETUP

To validate the working of our developed fNIRS and tDCS system we performed a very basic experiment described in [40]. Experiment was performed on three healthy male subjects (mean age 28.67 ± 5.2). All subjects had normal or corrected to normal vision. No subject had a history of any neurological or psychiatric disorders. All three subjects were right handed. Experiment was performed on individual subject while sitting on a comfortable seat. A verbal consent of the subjects was taken and the experiment was performed under the declaration of Helsinki.

The resting state data using newly developed fNIRS system was collected from prefrontal cortex in two conditions: before and after stimulation. Before stimulation, data was collected for 5 minutes whereas after stimulation a 10 minutes data was collected to properly check the stimulation effects. The position of fNIRS probe and the channel configuration is shown in Figure 5(a).

tDCS was provided by the newly developed tDCS system using saline-soaked sponge electrodes (having surface area of 35cm2). Electrodes were placed on the scalp of subjects' prefrontal cortex area. Anode was placed at the Fp1 and cathode was placed at Fp2 of the 10-20 international standards for EEG electrode placement.

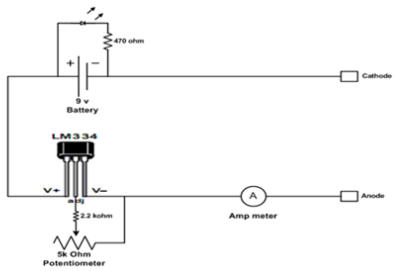

Figure 3. tDCS system circuit diagram

IV. RESULTS AND DISCUSSION

Figure 4 shows the time series fNIRS data. The data is averaged for 16 channels and all three subjects. It can be seen that before stimulation the data is very stable near the baseline. There are not many fluctuations during these 5 minutes which shows that there is not much activity during this time. After the first five minutes the next 10 minutes are in which stimulation is applied so during this time there is no fNIRS data recording. After the stimulation we can clearly see significant increase in HbO and decrease in HbR for about first four minutes and then it comes down and at the end of 10 minutes it tries to settle on the baseline. This increase in HbO and decrease in HbR shows that neurons are highly active during this period. The fNIRS data is collecting in the resting state of the subject so this activation of neurons is directly associated with the application of tDCS.

Our results are in accordance with the previous literature that the anodal tDCS can increase the concentration of HbO in the human brain after the stimulation. We will agree with the previous hypothesis given by [40] that anodal tDCS can increase the excitability of neurons and this extra activity needs extra oxygen to fulfill its tasks. fNIRS is a noninvasive and non-ionizing technique to measure the physiological parameters like tissue oxygenation changes and blood volume. fNIRS has an advantage over the other brain imaging techniques like fMRI, PET, SPECT that it can be built in small portable size and it is very cost effective. The portable fNIRS may prove useful for brain [41-43] and control applications [44-51].

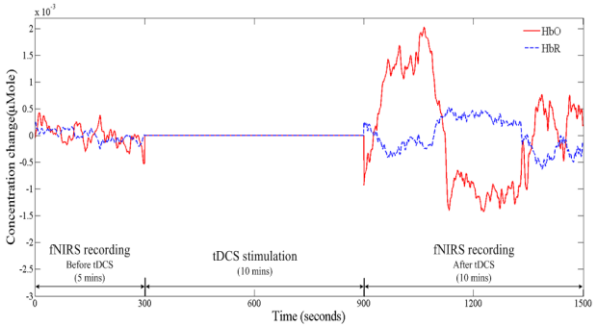

Figure 4. *Time series analysis of fNIRS data*

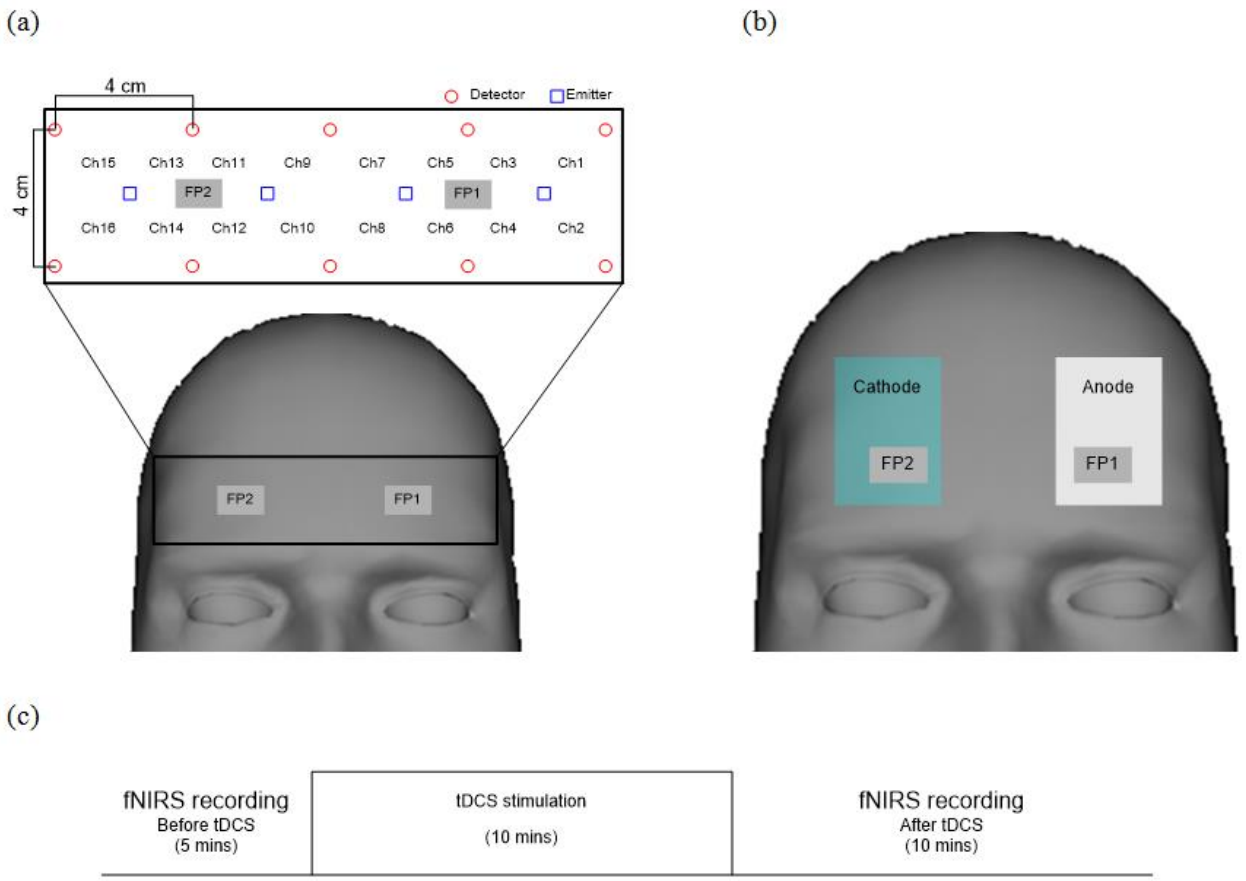

Figure 5. Experimental setup: (a) fNIRS probe position and channel configuration (b) tDCS electrode placement, (c) experimental paradigm

V. CONCLUSION

In this study we have developed a new fNIRS system with the flexible probe that can accommodate the sensors from EEG as well. Also we have developed a pad-type tDCS system with the variable current limits to test the effect of electric stimulation over the human brain. The functionality of individual system was tested first and then the combined experiment was performed with three male subjects to verify the working of both systems. The results obtained in this study are in accordance with the previous literature and show that an anodal tDCS with 1mA current for atleast 10 minutes excites the neurons under the region of interest and this excitability is recorded using the newly developed fNIRS system. This system will be useful to identify the patients with chronic cerebrovascular disorders and to increase the blood flow in the certain brain region of the patient.

REFERENCES

[1] Pascual-Leone, D. Bartres-Faz, J. P. Keenan, "Transcranial magnetic stimulation: studying the brain-behavior relationship by induction of 'virtual lesions'." *Philosophical Transactions of the Royal Society B: Biological Sciences*, vol. 354 no. 1387, pp.1229–1238, 1999.

[2] Priori, "Brain polarization in humans: a reappraisal of an old tool for prolonged noninvasive modulation of brain excitability." *Clinical Neurophysiology*, vol. 114, no. 4, pp. 589–595, 2003.

[3] T. Wagner, A. Valero-Cabre, A. Pascual-Leone, "Noninvasive human brain stimulation." *Annual Review of Biomedical Engineering*, vol. 15, no. 9, pp. 527-565, 2007.

[4] H. Santosa, M. J. Hong, S. P. Kim, and K.-S. Hong, "Noise reduction in functional near-infrared spectroscopy signals by independent component analysis," *Review of Scientific Instruments*, Vol. 84, no. 7, e073106, 2013.

[5] Gagnon, L. Desjardins-Crépeau, I. Tournier, M. Desjardins, F. Lesage, C. E. Greenwood, and L. Bherer, "Near-infrared imaging of the effects of glucose ingestion and regulation on prefrontal activation during dual-task execution in healthy fasting older adults," *Behavioral Brain Research*, vol. 232, no. 1, pp. 137-147, 2012.

[6] H. Santosa, M. J. Hong, and K.-S. Hong, "Lateralization of music processing with noises in the auditory cortex: an fNIRS study," *Frontiers in Behavioral Neuroscience*, vol. 8, e418, 2014.

[7] N. Naseer, K.-S. Hong, M. R. Bhutta and M. J. Khan, " Improving classification accuracy of covert yes/no response decoding using support vector machines: an fNIRS study," *Proc. of the IEEE International Conference on Robotics and Emerging Allied Technologies in Engineering (iCREATE),* pp. 6-9, 2014.

[8] M. R Bhutta, K.-S Hong, N. Naseer and M. J. Khan, "Water correction algorithm to improve the classification accuracy: a near-Infrared spectroscopy study," *Proc. of the IEEE International Conference on Robotics and Emerging Allied Technologies in Engineering (iCREATE)*, pp. 91-94, 2014.

[9] M. J. Khan, K.-S Hong, M. R Bhutta and N. Naseer, " Dual movement control command generation using prefrontal brain activity," *Proc. of the IEEE International Conference on Robotics and Emerging Allied Technologies in Engineering (iCREATE)*, pp. 244-248, 2014.

[10] N. Naseer, K.-S. Hong, M. J. Khan and M. R. Bhutta, "Classification of prefrontal and motor cortex activities for development of three-class fNIRS-BCI," *20th Annual Meeting of the Organization for Human Brain Mapping (OHMB)*, 2014.

[11] N. Naseer, and K.-S. Hong, "Decoding answers to four-choice questions using functional near infrared spectroscopy," *Journal of Near Infrared Spectroscopy*, vol. 23, no. 1, pp. 23-31, 2015.

[12] M. J. Khan, K.-S Hong, N. Naseer and M. R. Bhutta, "Multi-decision detection using EEG-NIRS based hybrid brain-computer interface

(BCI)," *20th Annual Meeting of the Organization for Human Brain Mapping (OHMB)*, 2014.

[13] M. R. Bhutta, and K.-S. Hong, "Water Correction Algorithm to Increase the Signal Strength of Oxy and Deoxy- Hemoglobin in Near-Infrared Spectroscopy Signals," *Proc. of the IEEE International Conference on Industrial Technology (ICIT)*, pp. 589-593, 2014.

[14] M. J. Khan, K.-S Hong, N. Naseer, M. R. Bhutta, "A hybrid brain-computer interface based on common EEG and NIRS resting state for BCI" *Proc. of the 14th International Conference on Control, Automation and Systems (ICCAS)*, pp. 275-278, 2014.

[15] M. J. Khan, K.-S Hong, N. Naseer, M. R. Bhutta, S. H. Yoon, "Hybrid EEG-NIRS BCI for rehabilitation using different brain signals," *Proc. of the Annual Conference of the Society of Instrument and Control Engineers (SICE)*, pp. 1768-1773, 2014.

[16] X. S. Hu, K.-S. Hong, and S. S. Ge, "Recognition of stimulus-evoked neuronal optical response by identifying chaos levels of near-infrared spectroscopy time series," *Neuroscience Letters*, vol. 504, no. 2, pp. 115-120, 2011.

[17] K. Kim, S. Lee, D. Koh, and B.-M. Kim, "Development of wireless NIRS system with dynamic removal of motion artifacts," *Biomedical Engineering Letters*, vol. 1, no. 4, pp. 254-259, 2011.

[18] M. R. Bhutta, and K.-S. Hong, "A new near-infrared spectroscopy system for detection of hemoglobin and water concentration changes during a human activity," *Proc. of the International Conference on Robotics, Biomimetics, Intelligent Comput. Syst. (ROBIONETICS)*, pp. 224-227, 2013.

[19] M. R. Bhutta, K.-S. Hong, B.-M. Kim, M. J. Hong, Y.-H. Kim, and S.-H. Lee, "Note: Three wavelengths near-infrared spectroscopy system for compensating the light absorbance by water," *Review of Scientific Instruments*, vol. 85, no. 2, e026111, 2014.

[20] V. Quaresima, R. Lepanto, and M. Ferrari, "The use of near infrared spectroscopy in sports medicine," *Journal of Sports Medicine and Physical Fitness*, vol. 43, no. 1, pp. 1-13, 2003.

[21] M. C. Taillefer, and A. Y. Denault, "Cerebral near-infrared spectroscopy in adult heart surgery: systematic review of its clinical efficacy," *Canadian Journal of Anesthesia*, vol. 52, no. 1, pp. 79-87, 2005.

[22] M. R Bhutta, K.-S Hong, N. Naseer and M. J. Khan, "Classification of lie and truth in forced choice paradigm: an fNIRS study," *Proc. of the 20th Annual Meeting of the Organization for Human Brain Mapping (OHMB)*, 2014.

[23] M. R. Bhutta, and K.-S. Hong, "Classification of fNIRS signals for deception decoding using LDA and SVM," *Proc. of the IEEE 13th International Conference on Control, Automation and Systems (ICCAS)*, pp. 1776-1780, 2013.

[24] M. R. Bhutta, M. J. Hong, Y.-H. Kim, and K.-S. Hong, "Single-trial lie detection using a combined fNIRS-polygraph system," *Frontiers in Psychology*, vol. 6, e709, 2015.

[25] N. Naseer, and K.-S. Hong, "Classification of functional near-infrared spectroscopy signals corresponding to the right-and left-wrist motor imagery for development of a brain–computer interface," *Neuroscience Letters*, vol. 553, pp. 84-89, 2013.

[26] K.-S. Hong, N. Naseer, and Y,-H. Kim, "Classification of prefrontal and motor cortex signals for three-class fNIRS-BCI," *Neuroscience Letters*, vol. 587, pp. 87-92, 2015.

[27] N. Naseer, M. J. Hong, and K.-S. Hong, "Online binary decision decoding using functional near-infrared spectroscopy for the development of brain–computer interface," *Experimental Brain Research*, vol. 232, no. 2, pp. 555-564, 2014.

[28] N. Naseer, and K.-S. Hong, "fNIRS-based brain-computer interfaces: a review," *Frontiers in Human Neuroscience*, vol. 9, e3, 2015.

[29] M. R. Bhutta, K.-S. Hong, N. Naseer, M. J. Khan, "Hemodynamic signals based lie detection using a new wireless NIRS system," *Proc. of the Annual Conference of the Society of Instrument and Control Engineers (SICE)*, pp. 979-984, 2014.

[30] T. Muehlemann, D. Haensse, and M. Wolf, "Wireless miniaturized in-vivo near infrared imaging," *Optics Express*, vol. 16, no. 14, pp. 10323-10330, 2008.

[31] M. J. Khan, M. J. Hong, and K.-S. Hong, "Decoding of four movement directions using hybrid NIRS-EEG brain-computer interface," *Frontiers in Human Neuroscience*, vol. 8, e244, 2014.

[32] K.-S. Hong, and N. Naseer, "Reduction of delay in detecting initial dips from functional near-infrared spectroscopy signals using vector-based phase analysis," *International Journal of Neural Systems*, vol. 26, no. 3, 1650012, 2016.

[33] M. J. Khan, and K.-S. Hong, "Passive BCI based on drowsiness detection: an fNIRS study," *Biomedical Optics Express*, vol. 6, no. 10, pp. 4063-4078, 2015.

[34] K.-S. Hong, and H. Santosa, "Decoding four different sound-categories in auditory cortex using functional near-infrared spectroscopy," *Hearing Research*, vol 333, pp. 157-166, 2016.

[35] Y. Lin, G. Lech, S. Nioka, X. Intes, and B. Chance, "Noninvasive, low-noise, fast imaging of blood volume and deoxygenation changes in muscles using light-emitting diode continuous-wave imager," *Review of Scientific Instruments*, vol. 73, no. 8, pp. 3065-3074, 2002.

[36] Z. Zhang, B. Sun, H. Gong, L. Zhang, J. Sun, B. Wang, and Q. Luo, "A fast neuronal signal-sensitive continuous-wave near-infrared imaging system," *Review of Scientific Instruments*, vol. 83, no. 9, e094301, 2012.

[37] L. Kocsis, P. Herman, and A. Eke, "The modified Beer–Lambert law revisited," Physics in Medicine and Biology, vol 51, no. 5, e91, 2006.

[38] F. Scholkmann, and M. Wolf, "General equation for the differential pathlength factor of the frontal human head depending on wavelength and age," *Journal of Biomedical Optics*, vol. 18, no. 10, e105004, 2013.

[39] UCL Department of Medical Physics and Bioengineering, "Specific Extinction Spectra of Tissue Chromophores," http://www.ucl.ac.uk/medphys/research/borl/intro/spectra

[40] C. Merzagora, G. Foffani, I. Panyavin, L. Mordillo-Mateos, J. Aguilar, B. Onaral, and A. Oliviero, "Prefrontal hemodynamic changes produced by anodal direct current stimulation," *Neuroimage*, vol. 49, no. 3, pp.2304-2310, 2010.

[41] M. A. Kamran, and K.-S. Hong, "Reduction of physiological effects in fNIRS waveforms for efficient brain-state decoding," *Neuroscience Letters*, vol. 580, pp. 130-136, 2014.

[42] K.-S. Hong, and H.-D. Nguyen, "State-space models of impulse hemodynamic responses over motor, somatosensory, and visula cortices," *Biomedical Optics Express*, Vol. 5, No. 6, pp. 1778-1798, 2014.

[43] M. Rehan, and K.-S. Hong, "Modeling and automatic feedback control of tremor: adaptive estimation of deep brain stimulation," *PLoS One*, vol. 8, no. 4, e62888, 2013.

[44] U. H. Shah, and K.-S. Hong, "Input shaping control of a nuclear power plant's fuel transport system," *Nonlinear Dynamics*, vol. 77, no. 4, pp. 1737-1748, 2014.

[45] A. K. Pamosoaji, P. T. Cat, and K.-S. Hong, "Sliding-mode and proportional-derivative-type motion control with radial basis function neural network based estimator for wheeled vehicles," *International Journal of Systems Science*, vol. 45, no. 12, pp. 2515-2528, 2014.

[46] A. Widyotriatmo, and K.-S. Hong, "A navigation function-based control of multiple wheeled vehicles," *IEEE Transactions on Industrial Electronics*, vol. 58, no. 5, pp. 1896-1906, 2011.

[47] K.-S. Hong, H. C. Sohn, and J. K. Hedrick, "Modified skyhook control of semi-active suspensions: A new model, gain scheduling, and hardware-in-the-loop tuning," *ASME Transactions, Journal of Dynamic Systems*, Measurement, and Control, vol. 124, no. 1, pp. 158-167, 2002.

[48] K.-S. Hong and J. Bentsman, "Direct adaptive control of parabolic systems: Algorithm synthesis, and convergence and stability analysis," *IEEE Transactions on Automatic Control*, vol. 39, no. 10, pp. 2018-2033, 1994.

[49] K.-S. Hong, K. H. Choi, J. G. Kim, and S. Lee, "A PC-based open robot control system: PC-ORC," *Robotics and Computer-Integrated Manufacturing*, vol. 17, no. 4, pp. 355-365, 2001.

[50] K.-J. Yang, K.-S. Hong, and F. Matsuno, "Robust adaptive boundary control of an axially moving string under a spatiotemporally varying tension," *Journal of Sound and Vibration*, vol. 273, no. 4-5, pp. 1007-1029, 2004.

[51] H. Park, D. Chwa, and K.-S. Hong, "A feedback linearization control of container cranes: Varying rope length," *International Journal of Control, Automation, and Systems*, vol. 5, no. 4, pp. 379-387, 2007.